Food & Function

ROYAL SOCIETY OF CHEMISTRY

PAPER

View Article Online
View Journal | View Issue

Cite this: *Food Funct.*, 2025, **16**, 5822

Flavonoids of *Rosa sterilis* S. D. Shi improve high-fat diet-induced obesity in mice by inhibiting lipid accumulation and regulating the gut microbiota†

Rui-Xue Yu,‡[a,b] Xu-Lu Luo,‡[c] Ji-Qiu Wang,[a,b] Jiao-Jiao Li,[a] Hejiang Zhou,[a,b] Yong-He Li*[d] and Ling-Yan Su*[a,b]

Received 24th March 2025,
Accepted 9th June 2025

DOI: 10.1039/d5fo01469g

rsc.li/food-function

Obesity is a complex disease associated with poor dietary habits and the gut microbiota. *Rosa sterilis* S. D. Shi contains abundant flavonoids, which have significant antioxidant, anti-inflammatory, and anti-obesity effects. Flavonoids from *Rosa sterilis* S. D. Shi (FRS) are bioactive compounds with multiple activities. The aim of the present study was to investigate whether and how the FRS can alleviate high-fat diet (HFD)-induced obesity in mice. Our results suggested that there are significant reductions in obesity-related phenotypes after 12 weeks of FRS intervention in HFD-induced mice. FRS significantly reduced weight gain, minimized liver damage, and restored liver and epididymal fat morphology in mice with HFD. Furthermore, FRS increased the population of beneficial bacteria *Akkermansia*, which helped counteract obesity, thereby improving glucose homeostasis and reducing lipid accumulation by modulating the gut microbiota composition. In conclusion, as a non-toxic and biologically active natural ingredient, FRS has the potential to prevent obesity and related metabolic disorders, and is expected to become a functional ingredient for researching anti-obesity and improving consumer health. This study provides a theoretical foundation and technical support for developing functional FRS products and underscores the importance of FRS in anti-obesity research and the advanced utilization of *Rosa sterilis* S. D. Shi resources.

1. Introduction

An imbalanced diet can easily lead to fat accumulation and obesity, which can trigger a series of chronic metabolic diseases: such as hypertension, hyperlipidemia, hyperglycemia, atherosclerosis, coronary heart disease, and other cardiovascular and cerebrovascular diseases.[1] Currently, the most commonly used anti-obesity drugs on the market are chemically synthesized drugs (such as statins and beta-blockers with significant lipid-lowering effects), but their drug dependence and potential side effects limit their clinical application.[2] Therefore, searching for natural products with fewer anti-obesity side-effects has become more and more important. Natural products from plants are attractive due to their non-toxicity, health advantages and suitability as functional foods for prolonged diet.[3] Flavonoids are a large group of low molecular weight secondary metabolites produced by plant photosynthesis.[4] They have biological activities *in vivo* and *in vitro*, such as anti-oxidation, anti-atherosclerosis and blood lipid reduction.[4] Thus, plant-derived natural products may be important for developing novel potential anti-obesity therapeutic strategies.

Inhibition of cholesterol synthesis and fat absorption, promotion of cholesterol degradation, fatty acid oxidation and enhancement of metabolism can prevent obesity.[5,6] Gut microbiota imbalance is closely related to obesity, and previous studies have shown that increasing the number of beneficial bacteria can improve obesity.[7] The gut microbiota can also regulate cholesterol and lipid metabolism, thereby achieving the effect of reducing obesity.[8] A high-fat diet disrupts the antioxidant capacity and the balance of the gut microbiota. This ultimately leads to the loss of the body's natural protective barrier against pathogenic bacteria. This ecological imbalance further disrupts lipid metabolism, creating a vicious cycle that leads to obesity, inflammatory bowel disease, ulcerative colitis,

[a]*College of Food Science and Technology, Yunnan Agricultural University, Kunming, Yunnan 650201, China. E-mail: sulingyanlsq@126.com*
[b]*Yunnan Provincial Laboratory of Precision Nutrition and Personalized Manufacturing , Yunnan International Joint Laboratory of China-Cambodia Signature Agro-Products Green Development, Yunnan Agricultural University, Kunming, Yunnan 650201, China*
[c]*College of Landscape Architecture and Horticulture, Yunnan Agricultural University, Kunming 650201, China*
[d]*College of Plant Protection, Yunnan Agricultural University, Kunming 650201, China. E-mail: swfclyh@ynau.edu.cn*

†Electronic supplementary information (ESI) available. See DOI: https://doi.org/10.1039/d5fo01469g

‡These authors contributed equally to this work.

and other diseases This ecological imbalance further disrupts lipid metabolism, forming a vicious cycle that leads to obesity, inflammatory bowel disease, ulcerative colitis, and other diseases.[9] The gut microbiota may be a new target for the treatment of hyperlipidemia and obesity.

Rosa roxburghii Tratt, also known as the king of the mountain, *prickly berry*, and *prickly pineapple*, is a perennial deciduous shrub in the Rosaceae family.[10]*Rosa sterilis* S. D. Shi has a close genetic relationship with *Rosa roxburghii* Tratt.[11] It has certain preventive and therapeutic effects on scurvy, night blindness, cancer, hypertension, hyperlipidemia, and obesity. *Rosa sterilis* S. D. Shi is an edible wild fruit with a strong aroma and a slightly sour and astringent taste. It is rich in various nutrients such as vitamin C, superoxide dismutase (SOD), minerals, polysaccharides, flavonoids, phenolic compounds, triterpenoids, and organic acids.[12–14] As a traditional medicinal and food plant, *Rosa sterilis* S. D. Shi has high medicinal and food value. *Rosa sterilis* S. D. Shi has preventive and therapeutic effects against scurvy, night blindness, cancer, hypertension, hyperlipidemia and obesity.[15,16] Previous studies have shown that the aqueous extracts and polysaccharides of *Rosa roxburghii* Tratt can treat type 2 diabetes or reduce hyperlipidemia,[10,17] but the molecular mechanism is not clear. *Rosa sterilis* S. D. Shi is rich in various types of flavonoids,[18] known as the "king of flavonoids". As one of the main active components of *Rosa sterilis* S. D. Shi, flavonoids from *Rosa sterilis* S. D. Shi (FRS) make important contributions to health promotion.[19] There are few studies on the role of FRS in the prevention of obesity in animals and research on the regulation of the gut microbiota is still in its infancy. Considering the crucial role played by the gut microbiota in the development of obesity, we hypothesize that the gut microbiota regulated by FRS may play a pivotal role in this process.

In this study, we aim to investigate whether FRS has an anti-obesity effect and the possible molecular mechanism of this effect. Using HFD-induced mouse models, we demonstrated the active involvement of FRS in obesity. We uncovered the underlying mechanism that treatment with FRS restored the obesity phenotype by inhibiting lipid accumulation and regulating the gut microbiota. These novel findings provide the idea of looking for the characteristic microbiota related to obesity and the technical support and theoretical basis for the development of functional FRS products. This is very important for the study of the anti-obesity effect of FRS and the deep processing and valuable utilization of the *Rosa sterilis* S. D. Shi resource.

2. Materials and methods

2.1. Preparation of FRS

The fruits of *Rosa sterilis* S. D. Shi were collected from the planting base of *Rosa sterilis* S. D. Shi in Xingren County, Guizhou Province. The fruits were dried in a hot air oven at 50 °C for 24 h, then ground and sieved through an 80 mesh screen to obtain the required fruit powder. Enzyme-assisted and ultrasound extraction method: 50.0% ethanol, 50.0 mL g^{-1} liquid–solid ratio, 70.0 minutes extraction time, and 3.0% enzyme dosage. The mixture underwent enzymatic digestion in a 50 °C water bath for 60 min, followed by extraction with an ultrasonicator (SB25-12DTDS, Ningbo Scientz Biotechnology Co., Ltd, Ningbo, China) at 45 °C, 33 kHz, and 300 W. After extraction, the solution was centrifuged at 5000 rpm for 10 min. Subsequent purification of the extracted flavonoids using AB-8 macroporous resin, and higher purity and yield of *Rosa sterilis* S. D. Shi total flavonoids can be obtained through resin adsorption followed by desorption with 70% ethanol. The flow rate during this process was maintained at 2 BV h^{-1}. Finally, the total flavonoids in the purified product were freeze-dried into powder.

The analysis utilized an Agilent ultra-high-performance liquid chromatograph (1290 UPLC) linked to a QTOF6550 mass spectrometer, employing electrospray ionization in both positive and negative modes. The Waters BEH C18 chromatographic column (2.1 mm × 100 mm, 1.7 μm) was used to separate and detect flavonoids in the purified extracts of *Rosa sterilis* S. D. Shi. The temperature was maintained at 35 °C, with an injection volume of 5 μL and a flow rate of 0.3 mL min^{-1}. Mass spectrometry was conducted over a mass-to-charge (m/z) range of 100 to 1500, utilizing a gas flow rate of 12 L min^{-1}. Ionization voltages were set to 4000 V for positive mode and 3200 V for negative mode. Solvent A consisted of 0.1% HCOOH-H_2O, while solvent B was methanol, with the following elution gradient: 0–25 min (10–80% B), 25–27 min (80–85% B), 27–30 min (85–95% B), 30–32 min (95–100% B), 32–33 min (100–10% B), and 33–35 min (10% B). The basic information about FRS is summarized in a table (Table S1†).

2.2. Animal experiments

Male C57BL/6J mice, aged 6 to 8 weeks, were procured from Sibeifu (Beijing) Biology Technology Co., Ltd. The mice were kept in an environment where they had unrestricted access to food and water, maintained at a temperature of 22 ± 2 °C, with 50% humidity and a 12 hour light/dark cycle. Following a 7 day acclimatization period, the mice were randomly assigned to one of six groups, each consisting of 10 animals. The control group (CON) received a diet comprising 10% low-fat feed along with an equivalent amount of physiological saline administered by gavage. The high-fat diet model group (HFD) was provided with a 60% high-fat diet and also received the same volume of physiological saline *via* gavage. The low-dose FRS group (FRS25) was fed a 60% high-fat diet and given a daily oral dose of 25 mg kg^{-1} FRS solution. The medium-dose FRS group (FRS50) received a 60% high-fat diet along with an oral administration of 50 mg kg^{-1} FRS solution. Lastly, the high-dose FRS group (FRS100) was given a 60% high-fat diet and administered 100 mg kg^{-1} FRS solution daily at 13:00 for a duration of 12 weeks. Each group of mice was housed individually, with continuous access to food and water. The weights of mice were recorded daily, and their feed was replenished every two days. Additionally, the intake of food and water was monitored. Throughout the experiment, the physiological con-

ditions of the mice were carefully observed to assess any potential toxicity or side effects of FRS on their growth. All animal procedures were performed in accordance with the Guidelines for Care and Use of Laboratory Animals of Yunnan Agriculture of University and approved by the Animal Ethics Committee of Yunnan Agriculture of University (approval no: APYNAU202411006).

2.3. Feces and tissue preparation

Two days prior to the conclusion of gastric lavage, the mice were subjected to a 12 hour fasting period overnight, and their fasting blood glucose levels and oral glucose tolerance were assessed the following morning. Following the final gastric lavage, another 12 hour fast was implemented, during which fresh fecal samples were collected in sterile centrifuge tubes, frozen in liquid nitrogen, and subsequently stored at −80 °C for future analysis. At the end of the treatment cycle, all animals were euthanized by sodium pentobarbital overdose (60 mg kg^{-1}, intraperitoneally). Blood was obtained through cardiac puncture, and the mice were then perfused with ice-cold saline *via* the heart. The tissues were harvested on ice, weighed, and divided; one portion was fixed in a 4% paraformaldehyde solution, while the other was stored in a sterile centrifuge tube at −80 °C. For the blood samples, after standing at room temperature for 2 hours, they were centrifuged at 4 °C and 3000 rpm for 15 minutes to separate the supernatant, which was then stored at −80 °C for later use.

2.4. Determination of serum biochemical indicators

The collected mouse serum was removed from the −80 °C freezer, thawed on ice, and then subjected to centrifugation at 4 °C at 3000 rpm for 15 minutes. The supernatant was collected for the measurement of triglycerides (TG), total cholesterol (TC), low-density lipoprotein cholesterol (LDL-C), and high-density lipoprotein cholesterol (HDL-C) in the serum of each group of mice using a fully automated biochemical analyzer. Concurrently, the lipopolysaccharide (LPS) levels in the serum of each group were determined using the ELISA method according to the kit instructions (Jiangsu Meimian Industrial Co., Ltd, China). Additionally, the serum levels of liver function markers, alanine aminotransferase (ALT) and aspartate aminotransferase (AST) were assessed following the kit guidelines (Nanjing Jiancheng Bioengineering Institute, China).[20]

2.5. Measurement of liver biochemical indicators

The collected mouse liver was retrieved from the −80 °C freezer and thawed on ice. The liver was weighed and then homogenized in an ice bath according to the kit's specifications. After homogenization, the levels of TC and TG in the liver were measured following the protocol provided by Nanjing Jiancheng Bioengineering Institute, China.

2.6. Histopathological evaluation

The liver, epididymal fat, and pancreas were preserved in 4% neutral formalin and subsequently embedded in paraffin to achieve an approximate thickness of 4 μm (Wuhan Servicebio Technology Co., Ltd, China). Following dewaxing, the tissue samples were analyzed using light microscopy after hematoxylin–eosin (H&E) staining. Specimens of fixed liver and epididymal fat were sectioned using a cryostat for oil-red staining according to established protocols. Microscopy images of the liver, pancreas, and epididymal fat were captured through scanning, and the diameter of adipocytes as well as the number of crown-like structures per adipocyte area were quantified using ImageJ (Media Cybernetics, USA).[21]

2.7. 16S rDNA sequencing analysis of fecal microbiota

DNA was extracted from various samples using cetyltrimethylammonium bromide (CTAB) following the manufacturer's guidelines. This reagent is effective for isolating DNA from trace amounts of samples and is suitable for the preparation of DNA samples from most bacterial species. Nuclease-free water served as the blank control. The total DNA was eluted in 50 μL of elution buffer and stored at −80 °C until it was measured using PCR (LC-Bio Technology Co., Ltd, China).[22]

The PCR protocol for amplifying prokaryotic 16S fragments included an initial denaturation step at 98 °C for 30 seconds, followed by 32 cycles consisting of denaturation at 98 °C for 10 seconds, annealing at 54 °C for 30 seconds, and extension at 72 °C for 45 seconds. A final extension was performed at 72 °C for 10 minutes. The resulting PCR products were verified using 2% agarose gel electrophoresis. To eliminate the risk of false-positive PCR results, ultrapure water was utilized as a negative control throughout the DNA extraction procedure, instead of a sample solution. The PCR products were then purified with AMPure XT beads (Beckman Coulter Genomics, Danvers, MA, USA) and quantified using a Qubit (Invitrogen, USA). Amplicon pools were prepared for sequencing, and both the size and quantity of the amplicon library were evaluated using the Agilent 2100 Bioanalyzer (Agilent, USA) and the Library Quantification Kit from Illumina (Kapa Biosciences, Woburn, MA, USA), respectively. The sequencing of the libraries was carried out on the NovaSeq PE250 platform.

Paired-end reads were assigned to samples based on their unique barcode and truncated by cutting off the barcode and primer sequence. Paired-end reads were merged using FLASH. Quality filtering on the raw reads was performed under specific filtering conditions to obtain high-quality clean tags according to the fqtrim (v0.94). Chimeric sequences were filtered using Vsearch software (v2.3.4). After dereplication using DADA2, we obtained a feature table and feature sequence. Alpha diversity and beta diversity were randomly calculated by randomly normalizing to the same sequences. Then according to the SILVA (release 138) classifier, feature abundance was normalized using the relative abundance of each sample. Alpha diversity is applied in analyzing the complexity of species diversity for a sample through 5 indices, including Chao1, Observed species, Goods coverage, Shannon, Simpson, and all these indices in our samples were calculated using QIIME2. Beta diversity was calculated using QIIME2, and the graphs were drawn using the R package. Blast was used for sequence alignment, and the feature sequences were anno-

tated with the SILVA database for each representative sequence. Other diagrams were implemented using the R package (v3.5.2).

2.8. Statistical analysis

All experimental data are presented as the mean ± standard error (SEM). The statistical significance of variance was generated using one-way analysis of variance (ANOVA) with Tukey's *post-hoc* test using GraphPad Prism 8.0.2 software (GraphPad Software Inc., San Diego, CA, USA). Differences in body weight of mice from different groups in 12 weeks were determined using one-way ANOVA, followed by the least significant difference (LSD) *post hoc* test, as described in our previous study.[23] $^{*}P < 0.05$; $^{**}P < 0.01$; $^{***}P < 0.001$; $^{****}P < 0.0001$; ns, not significant.

3. Results

3.1. FRS improves obesity characteristics in mice fed with HFD

To explore the role of FRS in a HFD-induced obesity phenotype in mice, an obesity model was constructed by feeding male C57BL/6 mice a HFD for 12 weeks (Fig. 1A). After the animal experiment, the weight of mice (Fig. 1B), final body weight (Fig. 1C) and weight gain (Fig. 1D) in the HFD group were significantly higher than that in the CON group, and this effect could be counteracted by FRS (Fig. 1B–D). Meanwhile, from the liver weight, it can be seen that the HFD group had an increase in liver weight, while after FRS intervention, the liver weight significantly decreased (Fig. 1E), indicating that HFD increased weight gain and liver weight, while this effect was counteracted by FRS. Alanine aminotransferase (ALT) and aspartate aminotransferase (AST) mainly reflect the overall condition of liver function, including the presence of liver cell necrosis. The serum ALT content in the HFD group was significantly higher than that in the CON group (Fig. 1G), and the AST content was also higher than that in the CON group (Fig. 1H). FRS intervention reversed the increase of ALT and AST (Fig. 1G and 1H). These indicated that the mouse obesity model has been successfully established, induced by HFD, and FRS intervention can improve mouse weight, and liver function to a certain extent.

3.2. FRS attenuated hyperlipidemia and hyperglycemia in HFD-fed mice

HFD leads to obesity, which is often accompanied by abnormal blood lipids.[24] Our results showed that the serum TC had no significant change (Fig. 2A) in mice from different groups. The serum TG (Fig. 2B) and LDL-C (Fig. 2C) levels were significantly increased and the HDL-C (Fig. 2D) level was reduced in mice with HFD-fed compared to the CON group. Continuing to calculate LDL-C/HDL-C, it was found that the HFD group significantly increased (Fig. 2E), indicating that a high-fat diet has adverse effects on cardiovascular health. It was found that treatment with FRS could significantly reduce serum TG, LDL-C and LDL-C/HDL-C, and substantially increase HDL-C in mice fed with HFD (Fig. 2B–E). Lipopolysaccharide (LPS), also known as endotoxin, can also trigger HFD-induced insulin resistance.[25,26] Our result showed that HFD increased the serum content of LPS (Fig. 2F). At the same time, liver TC and TG were also detected, consistent with the serum lipid results, the content of liver TC (Fig. 2G) and TG (Fig. 2H) in the mice of the HFD group was significantly higher than those in the CON group, and the level of TG was significantly reduced after FRS intervention (Fig. 2H).

Obesity induced by a high-fat diet may cause abnormal glucose and lipid metabolism, which may easily lead to problems in islet function, insulin resistance, and other problems, and then lead to diabetes.[27] We found that HFD induced an increase in fasting blood glucose in mice, while FRS intervention significantly reduced fasting blood glucose in mice (Fig. 2I). After gavage of 2 g kg^{-1} glucose solution, the blood glucose levels of all three groups of mice reached their peak at 30 minutes, with the HFD group having the highest blood glucose levels, followed by a decreasing trend (Fig. 2J). The calculated area under the curve of the HFD group was significantly higher than the CON, and slightly higher than the HFD + FRS group (Fig. 2K). In addition, after 30 minutes, the HFD group showed a downward trend and ultimately remained higher than the CON and FRS groups at 120 minutes (Fig. 2J). In some cases, the enlargement of pancreatic islet cells may be associated with insulin resistance. Long term insulin resistance may lead to gradual impairment of pancreatic islet cell function, resulting in pathological changes such as pancreatic islet cell enlargement.[28] Then we performed the histopathological experiment to observe the pancreas, pancreatic tissue pathological sections demonstrated that HFD can cause pancreatic islet cell enlargement and initial insulin resistance (Fig. 2L and M). Meanwhile, FRS noticeably decreased the enlarged area of islets which was induced by HFD (Fig. 2L and M). These results indicate that long-term HFD intake may lead to glucose and lipid metabolism disorders, insulin resistance, and other conditions, and these effects could be reversed by FRS treatment.

3.3. FRS improved hepatic damage and fat accumulation of epididymal adipose tissue

The liver is essential for regulating energy metabolism, and any disruption in its energy processes can result in insulin resistance (IR) and oxidative stress.[29] H&E staining of liver tissue indicated that the HFD-fed group exhibited more pronounced vacuolar degeneration of liver cells, increased swelling of liver cells surrounding blood vessels, and a looser cytoplasmic structure compared to the CON group mice (Fig. 3A). FRS treatment significantly altered the liver cells, making them more similar to those in the CON group. Furthermore, Oil Red O staining revealed a substantial number of lipid droplets in the liver tissue of mice from the HFD group, while the liver tissues of the FRS and CON groups appeared relatively similar (Fig. 3A).

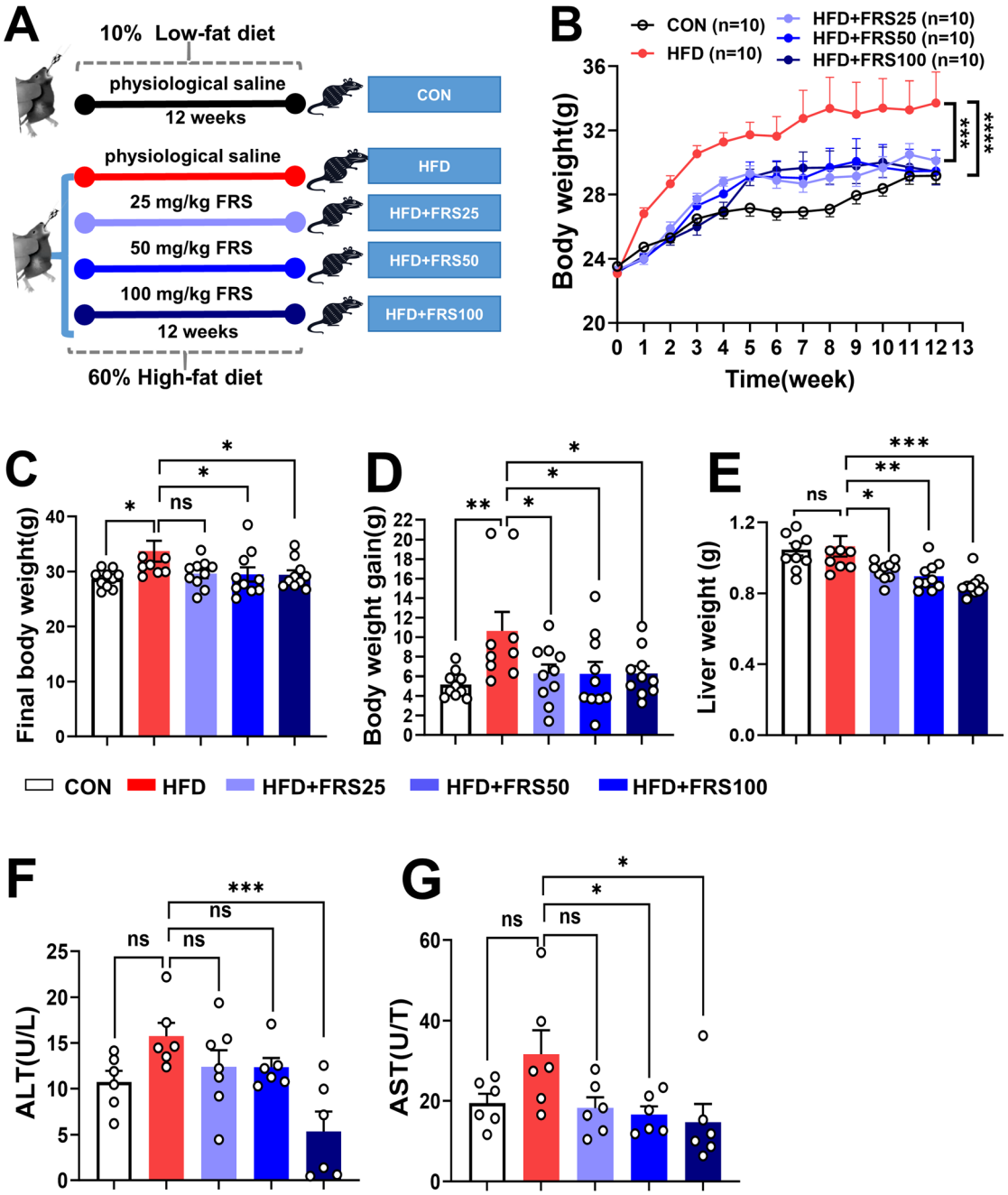

Fig. 1 HFD feeding induced an obesity mouse model and this effect can be reversed by FRS intervention. (A) The process of raising mice. (B) Changes in body weight of mice at 12 weeks. (C) Final body weight of mice from different groups. (D) Body weight gain of mice. (E) Liver weight of mice. (F) Serum alanine aminotransferase (ALT) of mice. (G) Serum aspartate aminotransferase (AST) of mice. The values are expressed as mean ± SEM (n = 6–10). Group differences were analyzed by one-way ANOVA with Tukey's *post-hoc* test. *P < 0.05; **P < 0.01; ***P < 0.001; ****P < 0.0001; ns, not significant.

Adipose tissue is a metabolic organ that stores energy, influences insulin, regulates glucose, and plays a role in inflammation.[30] The weight of epididymal fat was notably elevated in the group of mice that were fed a high-fat diet, while treatment with FRS significantly attenuated this effect (Fig. 3B). The adipocyte arrangement in the epididymal fat of the CON group is orderly and consistent, whereas the adipocyte arrangement in the HFD group is irregular and more pronounced (Fig. 3C). Additionally, the adipocytes in the HFD group are significantly larger than those in the CON group. Treatment with FRS resulted in a noticeable reduction in adipocyte size and a more organized arrangement (Fig. 3C). Measurements of adipocyte diameter revealed that both the diameter (Fig. 3D) and area (Fig. 3E) of adipocytes in the HFD

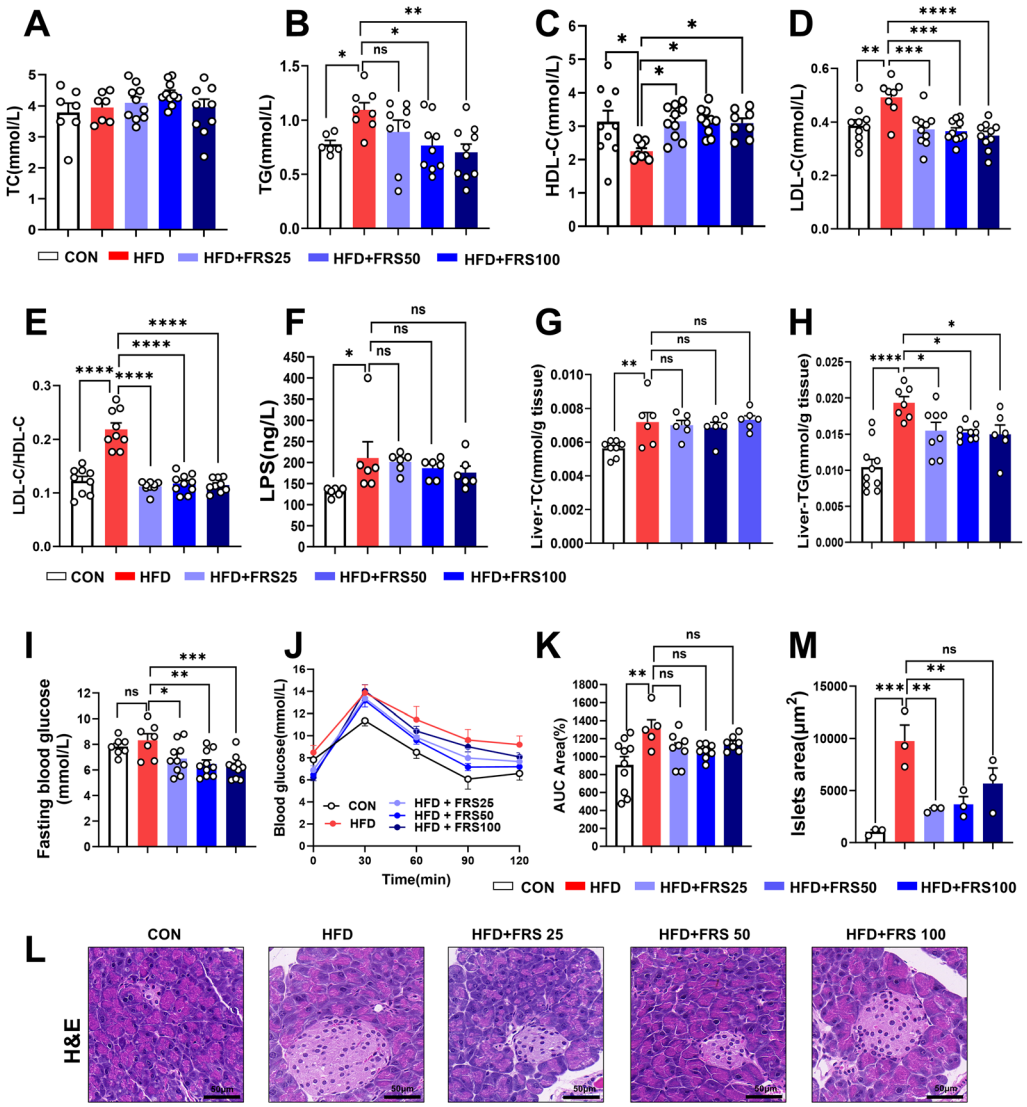

Fig. 2 FRS ameliorated high-fat diet-induced glucose metabolism and insulin resistance in mice. (A) Serum total cholesterol (TC). (B) Serum triglycerides (TG). (C) Serum low-density cholesterol (LDL-C). (D) Serum high-density cholesterol (HDL-C). (E) LDL-C/HDL-C. (F) Serum lipopolysaccharide (LPS). (G) Total cholesterol (TC) in the liver of mice from different groups. (H) Liver triglycerides (TG) of mice liver tissue. (I) 12 h fasting blood glucose of mice from different groups. (J) Changes in the oral glucose tolerance of mice from different groups. (K) Area under the oral glucose tolerance curve (AUC) of different groups. (L) H&E staining observation of pancreatic tissue of mice from different groups (40×, 50 μm). (M) Islet areas of mice. All results are presented as mean ± SEM (n = 6–10). Group differences were analyzed by one-way ANOVA with Tukey's *post-hoc* test. *P < 0.05; **P < 0.01; ***P < 0.001; ****P < 0.0001; ns, not significant.

group were significantly larger than those in the CON and FRS groups, and the coronal tissue area (Fig. 3F) was also markedly greater in the HFD group compared to the other two groups (Fig. 3C–F). Furthermore, we examined that the red O staining of epididymal fat indicated that the epididymal fat in the HFD group contained more red-stained lipid droplets, whereas the CON and FRS groups exhibited a relative decrease (Fig. 3G). Thus, we conclude that FRS intervention more effectively counteracted HFD-induced liver injury, lipid accumulation and adipocyte hypertrophy in mice. The safety and efficacy boundaries of FRS were analyzed by designing a gradient dose analysis. Based on the above indicators, it was determined that a medium dose of 50 mg kg^{-1} had a better effect. In the subsequent measurement of intestinal microbiota, we chose a medium dose of 50 mg kg^{-1} and named it HFD + FRS.

3.4. FRS restored the diversity and richness of the gut microbiota in HFD-induced mice

To investigate the impact of FRS intervention on the gut microbiota of mice fed a HFD, we conducted 16S rDNA sequencing on their fecal samples. Initially, we assessed the species diversity of the fecal microbiota. Our analysis revealed 498 common operational taxonomic units (OTUs) shared among the feces of the CON, HFD, and HFD + FRS groups, alongside 591 unique

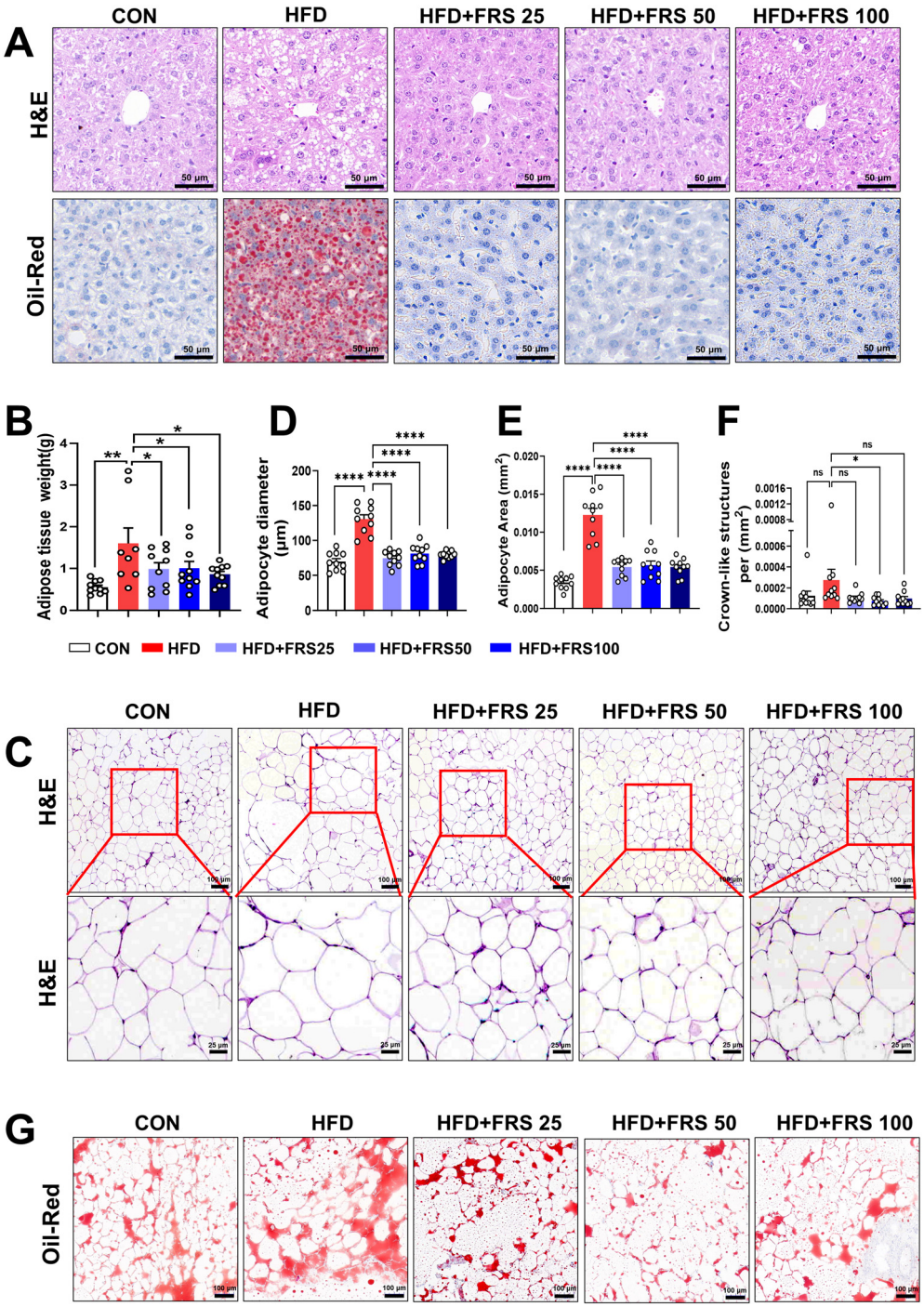

Fig. 3 FRS decreased fat mass and adipocytes enlarged by high-fat diet in mice. (A) Representative images of hematoxylin and eosin (H&E) and oil red O staining sections of mouse livers from control, HFD and FRS + HFD groups (bar = 50 μm). (B) Tissue weights of epididymal white adipose tissue (eWAT) of mice from different groups. (C) Representative images of H&E-stained sections of mouse eWAT in each group. (D) Quantifications of the adipocyte diameter and crown-like structures (CLS) of eWAT from B (n = 10). (E) Quantification of crown-like structures (CLS) of eWAT from B (n = 10). (F) Quantifications of the adipocyte area of eWAT (n = 10) from B. (G) Representative oil red O staining images of mature adipocytes of eWAT from mice with different treatments. All results are presented as mean ± SEM (n = 6–10). Group differences were analyzed by one-way ANOVA with Tukey's *post-hoc* test. *P < 0.05; ****P < 0.0001; ns, not significant.

OTUs from the CON group, 430 unique OTUs from the HFD group, and 1283 unique OTUs from the HFD + FRS group (Fig. 4A). This suggests that FRS treatment enhances the OTU diversity in mouse feces. The Chao1 and observed species indices, which primarily reflect the number of species within the community, represent the alpha diversity of the fecal

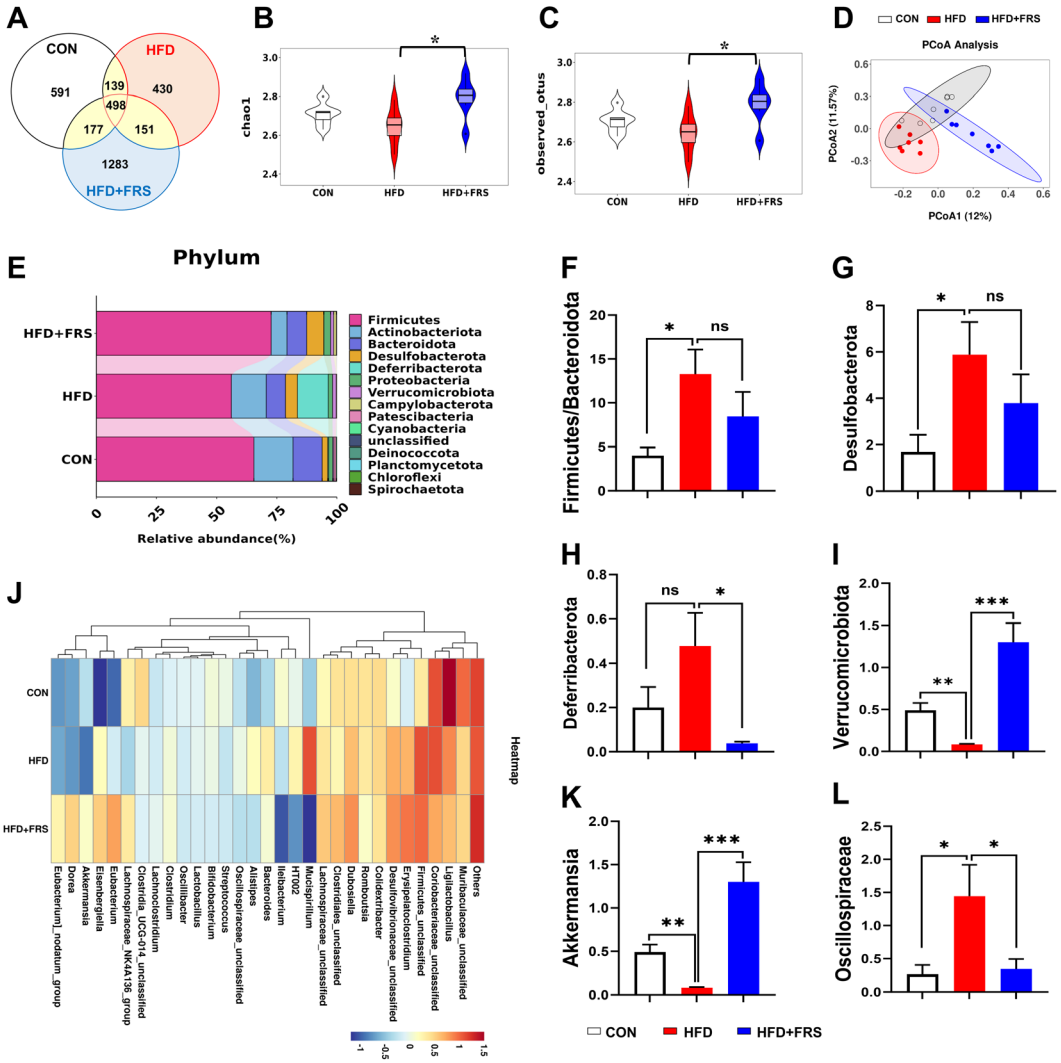

Fig. 4 FRS can reverse the gut microbiota dysbiosis induced by HFD. (A) Venn plot. (B) Chao1 index. (C) Observed-otus index. (D) Principal coordinates analysis of the gut microbiota (PCoA). (E) The effect of FRS on the gut microbiota composition in HFD fed mice at the phylum level. (F) The relative abundance of Firmicutes/Bacteroidetes, (G) Desulfobacterota, (H) Deferribacterota and (I) Verrucomicrobiota in mice from different groups. (J) The effect of FRS on the gut microbiota composition in HFD fed mice at the genus level. (K) The relative abundance of Akkermansia and (L) Oscillospiraceae in mice from different groups. All results are presented as mean ± SEM. Group differences were analyzed by one-way ANOVA with Tukey's *post-hoc* test. *$p < 0.05$; **$p < 0.01$; ***$p < 0.001$; ns, not significant.

microbiota. The Chao1 (Fig. 4B) and Observed-OTUs (Fig. 4C) indices were diminished in the microbiota of HFD mice; however, FRS intervention appeared to ameliorate this reduction. Additionally, we employed principal coordinate analysis (PCoA) using the weighted Unifrac method to visually evaluate the beta diversity of the fecal microbiota.[31] A notable separation was found among the HFD and HFD + FRS groups (Fig. 4D). These findings imply that FRS intervention positively influences the richness, diversity, and evenness of the gut microbiota.

3.5. FRS regulates gut microbiota dysbiosis induced by HFD in mice

Taxonomic analysis identified variations in the predominant gut microbiota among the different groups.[32] Phylum analysis indicated that the gut microbiota is composed of several phyla, including Bacteroidetes, Firmicutes, and Verrucomicrobia, among others (Fig. 4E). The abundance of Firmicutes/Bacteroidetes, which was considered a characteristic of obesity,[33] was significantly elevated in mice on a HFD compared to the CON group (Fig. 4F). Additionally, the abundance of Desulfobacterota (Fig. 4G) and Deferribacterota (Fig. 4H) was higher in the HFD group compared to the CON group. FRS intervention was able to restore the abundance of Firmicutes/Bacteroidetes, Desulfobacterota, and Deferribacterota (Fig. 4F–H). Conversely, Verrucomicrobia, which is negatively correlated with intestinal health,[34] was found to be reduced in the HFD group. However, the HFD + FRS group exhibited a significant increase in Verrucomicrobia compared to the HFD group (Fig. 4I).

At the genus level (Fig. 4J), the genus *Akkermansia*, a notable representative of Verrucomicrobiota, exhibited a reduction in the abundance associated with obesity.[34] Our findings revealed that HFD-fed mice had a decreased abundance of *Akkermansia*; however, treatment with FRS led to a significant increase in its abundance (Fig. 4K). Conversely, the population of Oscillospiraceae was markedly elevated in HFD-fed mice, but this increase was reversible following treatment with FRS (Fig. 4L). These findings suggested that FRS modulates the gut microbiota composition in HFD-fed mice, aligning it more closely with that of CON-fed mice. LEfSe analysis highlighted significant differences in gut microbiota taxa from the phylum to genus levels across the various groups. Among the five identified taxa, we found 59 distinct taxonomic groups (LDA > 3.3), including 16 genera. The CON group was characterized by genera such as Ligilactobacillus, *Ileibacterium*, Coriobacteriaceae, UCG002, and *Flavonifractor*. In contrast, the HFD group was identified with *Mucispirillum*, *Akkermansia*, and *Faecalibaculum* at the genus level. The HFD + FRS group primarily comprised *Erysipelatoclostridium*, *Eubacteria*, *Dorea*, Lachnospiraceae NK4A136_group, *Helicobacter*, *Ruminococcus torques*_group, *Parabacterioids*, UBA1819, and Rikenellaceae RC9_gut_group (Fig. 5A and B). Thus, these alterations in bacterial populations may indicate the pathogenesis linked to HFD-induced obesity.

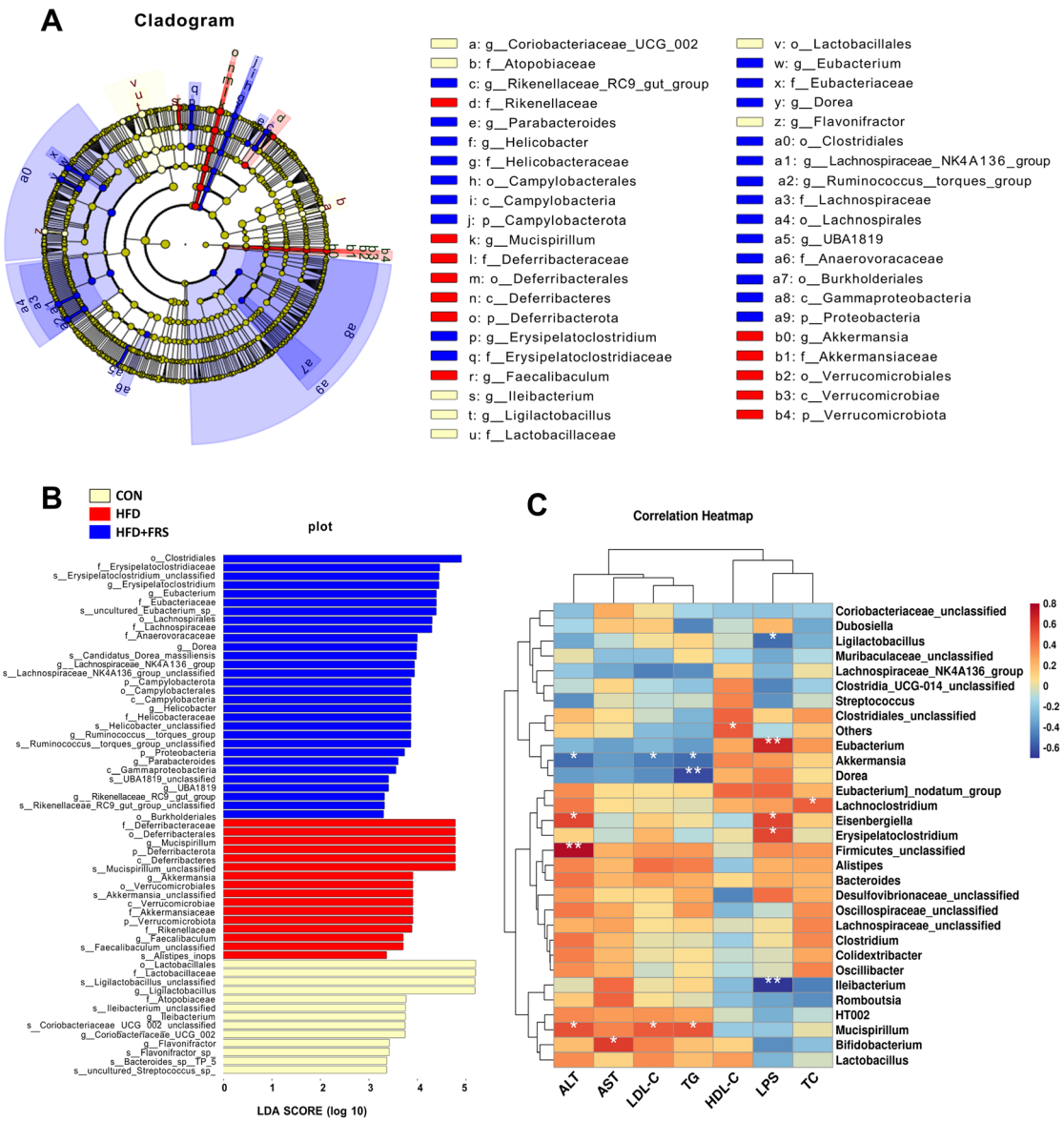

Fig. 5 Linear discriminant analysis (LDA) effect size (LEfSe) to identify the most significant taxonomic groups between CON, HFD, and FRS groups and Spearman correlation analysis. (A) The evolutionary branch diagram output by LEfSe analysis has an LDA score threshold set to 3.3. (B) The distribution bar chart of the LEfSe analysis output. (C) Spearman correlation analysis between the top 30 microbial communities at the genus level and obesity-related parameters. Group differences were analyzed by one-way ANOVA with Tukey's *post-hoc* test ($n = 6$). *$p < 0.05$; **$p < 0.01$.

3.6. The correlation between the gut microbiota and obesity parameters in mice

To further investigate the relationship between gut microbiota and factors associated with obesity detection, we performed Spearman correlation analyses. *Akkermansia* predominantly demonstrates a negative correlation with biochemical indicators including ALT, TG, and LDL-C. *Ligilactobacillus* and *Ileibacterium* primarily exhibit negative correlations with LPS, while *Dorea* shows a significant negative association with TG. Conversely, *Eubacterium* is positively correlated with LPS; *Lachnoclostridium* is positively associated with TC; *Eisenbergiella* displays positive correlations with both ALT and LPS; *Erysipelatoclostridium* is positively related to LPS; unclassified Firmicutes shows a positive correlation with ALT; *Mucispirillum* exhibits positive correlations with ALT, LDL-C, and TG; and *Bifidobacterium* demonstrates a positive correlation with AST (Fig. 5C). Consequently, we conclude that increasing the population of *Akkermansia* bacteria through FRS treatment can effectively regulate metabolism, enhance the obesity phenotype, and suppress fat production and cholesterol synthesis. FRS mitigates HFD-induced obesity by modulating the gut microbiota.

4. Discussion

In recent years, overweight, obesity and type 2 diabetes are the main risk factors for the development of cardiovascular disease worldwide.[35] Obesity is a complex disease accompanied by low-grade inflammation, lipid metabolism disorders, insulin resistance, and adipocyte hypertrophy.[36] Most obesity control drugs have side effects, and plant extracts are popular as a daily diet due to their extremely low side effects and multi-target treatment. Previous studies have shown that *Rosa sterilis* S. D. Shi extract has beneficial effects in various diseases, including hypoglycemic and lipid-lowering.[37] At present, research on the anti-obesity effects of *Rosa sterilis* S. D. Shi is mainly focused on polysaccharides or fermented *Rosa sterilis* S. D. Shi juice.[37–39] The specific effects and potential mechanisms of FRS on hyperlipidemia are not fully understood. The gut microbiota plays a crucial role in the pathogenesis of diet-induced obesity and related metabolic disorders and it has been identified as a key target for treating metabolic diseases.[40] The gut microbiota is a key mediator for the metabolic benefits of dietary polyphenols. FRS, a polyphenolic substance, often cannot be absorbed in the small intestine due to its large molecular structure and accumulates in the large intestine, where the gut bacteria convert them. This process generates various compounds with higher bioavailability.[41] Therefore, we examined the effects of FRS on the gut microbiota in a mouse model of obesity. In this study, we found that FRS exhibited better hypolipidemic effects and improved gut microbiota dysbiosis by increasing beneficial bacteria and decreasing the harmful bacteria in an HFD-induced obesity mouse model (Fig. 6).

Weight and adipose tissue weight are the most intuitive indicators in anti-obesity experiments. During the develop-

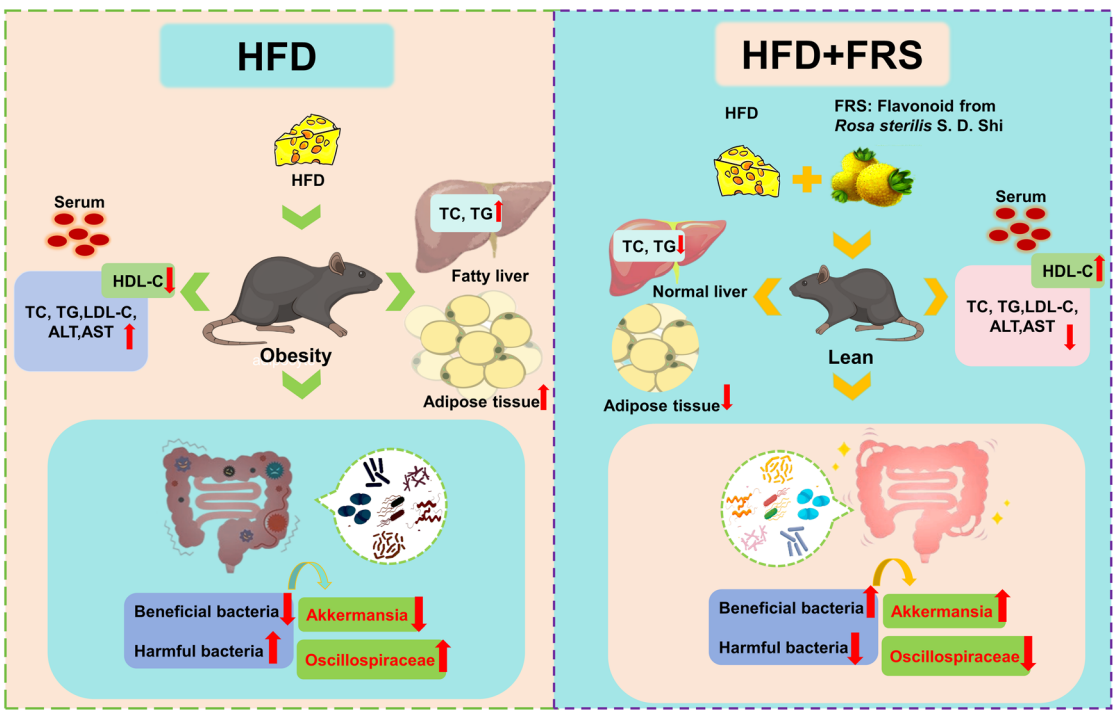

Fig. 6 Schematic of the potential mechanism underlying the effects of FRS on obesity. The improvement of lipid metabolism by FRS is achieved by regulating the composition of the gut microbiota, increasing the production of beneficial bacteria and reducing harmful bacteria, and improving glucose homeostasis, which has anti-obesity effects.

ment of HFD-induced obesity, lipids accumulate, preadipocytes differentiate, and mature adipocytes expand,[42] which will lead to lipid metabolism disorders accompanied by elevated levels of serum TC, TG, and LDL-C, as well as visceral obesity and injury.[43] Consistently, we found that FRS intervention reduced TG and LDL-C levels and increased HDL-C levels. High levels of blood sugar will eventually lead to diabetes.[44] HFD leads to elevated fasting blood glucose levels and dysregulated glucose homeostasis in mice, these effects could be reversed by FRS. In addition, the pancreas plays a crucial role in controlling blood glucose levels, and FRS treatment reduces pancreatic tissue lesions in mouse models.

Long-term overconsumption of HFD directly leads to excessive accumulation of energy and lipids, resulting in hyperlipidemia, insulin resistance, hyperglycemia, and chronic inflammation.[45] Consistent with previous studies,[29,39,46] our histopathologic results showed that HFD resulted in the production of large numbers of vacuoles and inflammatory infiltrates, as well as an increase in the number and volume of adipocytes in the liver tissues of mice. Meanwhile, treatment with FRS can reduce lipid accumulation, and visceral damage and partially improve lipid metabolism in HFD-fed mice accompanied by improved serum AST and liver TG levels. These results suggested that FRS could partly improve lipid metabolic disorders and visceral injury in HFD-fed mice.

The gut microbiota is affected by the diet and is widely recognized as a potential target for the treatment of obesity.[47] In the present study, we explored whether the beneficial effect of FRS in improving HFD-induced obesity is related to changes in the gut microbiota by using 16S sequencing analysis. FRS intervention can increase Chao1 and observed species indices in the microbiota of HFD induced mice, indicating that FRS had a positive effect on the richness and diversity of the gut microbiota. The increase in the proportion of Firmicutes/Bacteroidota (F/B) caused by HFD is considered a characteristic of obesity.[33] However, changes in the F/B ratio have varied in different studies,[48] and the influence of the gut microbiota on energy extraction is limited. In our study, we found that the abundance of Firmicutes increased and the abundance of Bacteroidetes decreased (meaning a higher F/B ratio) in HFD-fed mice, and this effect could be partly reversed by FRS treatment. FRS treatment also reversed the higher proportion of Deferribacterota and the lower proportion of Verrucomicrobia induced by HFD. These results indicate that FRS plays a beneficial role by regulating the proportion and diversity of the gut microbiota associated with the development of obesity.

In addition, FRS intervention increased the number of beneficial bacteria *Akkermansia* and inhibited the increase of harmful bacteria such as *Desulfovibrio* and Oscillospiraceae. The regulation effect of FRS on *Akkermansia* was not unexpected. Verrucomicrobiota is linked to gut health, regulating glucose and exhibiting anti-inflammatory effects. The abundance of Verrucomicrobiota is closely related to intestinal health, which contributes to regulating glucose homeostasis and has anti-inflammatory properties. *Akkermansia* is a type of Verrucomicrobiota, which was widely recognized as a star bacterium that can promote health through intestinal symbiosis.[49] A large number of studies have shown that the lack or decrease of *Akkermansia* is related to a variety of diseases, including obesity.[50]

Consistent with our mouse model results, *Akkermansia* was significantly reduced in the obese populations.[51] Moreover, Spearman correlation analysis conducted in this study showed that *Akkermansia* was mainly negatively correlated with indicators such as ALT, TG, and LDL-C. It can be seen that HFD leads to a decrease in the abundance of *Akkermansia*, while FRS increases the abundance of *Akkermansia*, playing a crucial role in combating obesity. FRS can regulate the gut microbiota and improve HFD-induced obesity by increasing the abundance of *Akkermansia*.

5. Conclusion

In summary, this study explored the alleviating effect and mechanism of FRS in obese mice induced by HFD. We found that treatment with FRS significantly attenuated body weight gain, blood lipids, and hyperlipidemia-related indicators, and restored the morphology of the liver and epididymal fat. Our results indicated that FRS exhibited its promising lipid-lowering effects, at least in part, by regulating lipid metabolism and the gut microbiota. However, further studies are required to identify the accurate bioactive anti-hyperlipidemic compounds in FRS and illustrate the causal relationships between these and the process of hyperlipidemia. Collectively, our results suggest that FRS has the potential to prevent obesity and related metabolic disorders and the promise of FRS as a functional ingredient for easing hyperlipidemia and improving public health.

Author contributions

Ling-Yan Su and Yong-He Li conceived and designed the experiments. Rui-Xue Yu, Xu-Lu Luo, Ji-Qiu Wang, Jiao-Jiao Li and Hejiang Zhou performed the experiments and analyzed the data. Ling-Yan Su and Rui-Xue Yu wrote the manuscript. Ling-Yan Su and Hejiang Zhou provided funding acquisition. All authors reviewed the content and approved the final version for publication.

Conflicts of interest

The authors declare that they have no known competing financial interests or personal relationships that could have appeared to influence the work reported in this paper.

Abbreviations

ALT Alanine aminotransferase
AST Aspartate aminotransferase

CLS	Crown-like structures
CON	Control
F/B	Firmicutes/Bacteroidota
FRS	Flavonoids of *Rosa sterilis* S. D. Shi
HDL-C	High-density lipoprotein cholesterol
HFD	High-fat diet
LDL-C	Low-density lipoprotein cholesterol
LPS	Lipopolysaccharides
OTUs	Operational classification units
qPCR	Quantitative real-time PCR
SOD	Superoxide dismutase
TC	Total cholesterol
TG	Triglycerides

Data availability

Data will be made available on request.

Acknowledgements

The study was performed at the Yunnan Agricultural University. It was supported the Applied Basic Research Foundation of Yunnan Province (202201AW070017 and 202401AS070091), the Yunnan Province-City Integration Project (202302AN360002), the Major Science and Technology Special Project Plan of Yunnan Province (202402AE090011), and the Yunnan Ten Thousand People Plan for Young Top Talents Project (YNWR-QNBJ-2018-378 and YNWR-QNBJ-2020-131).

References

1 J. Liu, J. Cai, P. Fan, X. Dong, N. Zhang, J. Tai and Y. Cao, Salidroside protects mice from high-fat diet-induced obesity by modulating the gut microbiota, *Int. Immunopharmacol.*, 2023, **120**, 110278–110289, DOI: 10.1016/j.intimp.2023.110278.

2 H. Mollazadeh, E. Tavana, G. Fanni, S. Bo, M. Banach, M. Pirro, S. von Haehling, T. Jamialahmadi and A. Sahebkar, Effects of statins on mitochondrial pathways, *J. Cachexia Sarcopenia Muscle*, 2021, **12**, 237–251, DOI: 10.1002/jcsm.12654.

3 B. Ahmad, E. P. Friar, M. S. Vohra, M. D. Garrett, C. J. Serpell, I. L. Fong and E. H. Wong, Mechanisms of action for the anti-obesogenic activities of phytochemicals, *Phytochemistry*, 2020, **180**, DOI: 10.1016/j.phytochem.2020.112513.

4 N. Shen, T. Wang, Q. Gan, S. Liu, L. Wang and B. Jin, Plant flavonoids: Classification, distribution, biosynthesis, and antioxidant activity, *Food Chem.*, 2022, **383**, 132531–132543, DOI: 10.1016/j.foodchem.2022.132531.

5 K. Nishida, S. Ueno, Y. Seino, S. Hidaka, N. Murao, Y. Asano, H. Fujisawa, M. Shibata, T. Takayanagi, K. Ohbayashi, Y. Iwasaki, K. Iizuka, S. Okuda, M. Tanaka, T. Fujii, T. Tochio, D. Yabe, Y. Yamada, Y. Sugimura, Y. Hirooka, Y. Hayashi and A. Suzuki, Impaired Fat Absorption from Intestinal Tract in High-Fat Diet Fed Male Mice Deficient in Proglucagon-Derived Peptides, *Nutrients*, 2024, **16**, 2270, DOI: 10.3390/nu16142270.

6 J. Yan, Q. Xue, W. Chen, K. Wang, D. Peng, J. Jiang, P. Li and B. Du, Probiotic-fermented rice buckwheat alleviates high-fat diet-induced hyperlipidemia in mice by suppressing lipid accumulation and modulating gut microbiota, *Food Res. Int.*, 2022, **155**, 111125–111136, DOI: 10.1016/j.foodres.2022.111125.

7 H.-Y. Li, S.-Y. Huang, D.-D. Zhou, R.-G. Xiong, M. Luo, A. Saimaiti, M.-K. Han, R.-Y. Gan, H.-L. Zhu and H.-B. Li, Theabrownin inhibits obesity and non-alcoholic fatty liver disease in mice via serotonin-related signaling pathways and gut-liver axis, *J. Adv. Res.*, 2023, **52**, 59–72, DOI: 10.1016/j.jare.2023.01.008.

8 H. Xu, F. Fang, K. Wu, J. Song, Y. Li, X. Lu, J. Liu, L. Zhou, W. Yu, F. Yu and J. Gao, Gut microbiota-bile acid crosstalk regulates murine lipid metabolism via the intestinal FXR-FGF19 axis in diet-induced humanized dyslipidemia, *Microbiome*, 2023, **11**, 262, DOI: 10.1186/s40168-023-01709-5.

9 Y. Ma, X. Zhang, B. Xuan, D. Li, N. Yin, L. Ning, Y.-L. Zhou, Y. Yan, T. Tong, X. Zhu, X. Huang, M. Hu, Z. Wang, Z. Cui, H. Li, J. Wang, J.-Y. Fang, R. Liu, H. Chen and J. Hong, Disruption of CerS6-mediated sphingolipid metabolism by FTO deficiency aggravates ulcerative colitis, *Gut*, 2024, **73**, 268–281, DOI: 10.1136/gutjnl-2023-330009.

10 C. Yin, Y. Zhang, L. Zhang, Y. Tian, X. Zhong, X. Fang, Y. Yang and A. Tao, Exploring Rosa roxburghii Tratt polysaccharides: From extraction to application potential in functional products - An in-depth review, *Int. J. Biol. Macromol.*, 2024, **280**, 135543, DOI: 10.1016/j.ijbiomac.2024.135543.

11 S. Chen, L. Luan, Y. Zhang, F. Liu, X. Ye and Z. Hou, A comparison study on polysaccharides extracted from Rosa sterilis S.D.Shi using different methods: Structural and in vitro fermentation characterizations, *Food Chem.: X*, 2023, **17**, 100533, DOI: 10.1016/j.fochx.2022.100533.

12 Y. Luo, R. Tang, H. Qiu and A. Song, Widely targeted metabolomics-based analysis of the impact of L. plantarum and L. paracasei fermentation on rosa roxburghii Tratt juice, *Int. J. Food Microbiol.*, 2024, **417**, 110686, DOI: 10.1016/j.ijfoodmicro.2024.110686.

13 Y. Zhang, X. Bian, G. Yan, B. Sun, W. Miao, M. Huang, N. Li and J.-L. Wu, Discovery of novel ascorbic acid derivatives and other metabolites in fruit of Rosa roxburghii Tratt through untargeted metabolomics and feature-based molecular networking, *Food Chem.*, 2023, **405**, 134807, DOI: 10.1016/j.foodchem.2022.134807.

14 L. Luan, H. Pan, Y. Chen, X. Ye, Z. Hou and S. Chen, Role of extracted phytochemicals from Rosa sterilis S. D. Shi in DSS-induced colitis mice: potential amelioration of UC, *Food Funct.*, 2023, **14**, 8369–8382, DOI: 10.1039/d3fo02456c.

15 C. Shen, Y. Wang, H. Zhang, W. Li, W. Chen, M. Kuang, Y. Song and Z. Zhong, Exploring the active components

and potential mechanisms of Rosa roxburghii Tratt in treating type 2 diabetes mellitus based on UPLC-Q-exactive Orbitrap/MS and network pharmacology, *Chin. Med.*, 2023, **18**, 12–27, DOI: 10.1186/s13020-023-00713-z.

16 G. Chen, M. Sun, K. Chen, L. Wang and J. Sun, Ultrasonic-Assisted Decoloration of Polysaccharides from Seedless Chestnut Rose (Rosa sterilis) Fruit: Insight into the Impact of Different Macroporous Resins on Its Structural Characterization and In Vitro Hypoglycemic Activity, *Foods*, 2024, **13**, 1349, DOI: 10.3390/foods13091349.

17 X. Li, Y. Ling, X. Huang, T. Zhou, S. Wu, S. Zhang, H. Zhou, Y. Kang, L. Wang, X. Wang and W. Yin, Rosa Roxburghii Tratt Fruit Extract Prevents Dss-Induced Ulcerative Colitis in Mice by Modulating the Gut Microbiota and the IL-17 Signaling Pathway, *Nutrients*, 2023, **15**, 4560, DOI: 10.3390/nu15214560.

18 J. Liu, C. Li, G. Ding and W. Quan, Artificial Intelligence Assisted Ultrasonic Extraction of Total Flavonoids from Rosa sterilis, *Molecules*, 2021, **26**, 3835, DOI: 10.3390/molecules26133835.

19 A. Jain, S. Sarsaiya, Q. Gong, Q. Wu and J. Shi, Chemical diversity, traditional uses, and bioactivities of Rosa roxburghii Tratt: A comprehensive review, *Pharmacol. Ther.*, 2024, **259**, 108657–108669, DOI: 10.1016/j.pharmthera.2024.108657.

20 Z. Guo, B. Hu, L. Zhu, Y. Yang, C. Liu, F. Liu, Y. Shi, M. Li, Z. Gu, Y. Xin, D. Yi, H. Liu and L. Zhang, Microbiome-metabolomics insights into the feces of high-fat diet mice to reveal the anti-obesity effects of yak (Bos grunniens) bone collagen hydrolysates, *Food Res. Int.*, 2022, **156**, 111024, DOI: 10.1016/j.foodres.2022.111024.

21 W. Ke, K. J. Flay, X. Huang, X. Hu, F. Chen, C. Li and D. A. Yang, Polysaccharides from Platycodon grandiflorus attenuates high-fat diet induced obesity in mice through targeting gut microbiota, *Biomed. Pharmacother.*, 2023, **166**, 115318–115332, DOI: 10.1016/j.biopha.2023.115318.

22 J. B. Logue, C. A. Stedmon, A. M. Kellerman, N. J. Nielsen, A. F. Andersson, H. Laudon, E. S. Lindström and E. S. Kritzberg, Experimental insights into the importance of aquatic bacterial community composition to the degradation of dissolved organic matter, *ISME J.*, 2016, **10**, 533–545, DOI: 10.1038/ismej.2015.131.

23 L.-Y. Su, L. Jiao, Q. Liu, X. Qiao, T. Xie, Z. Ma, M. Xu, M.-S. Ye, L.-X. Yang, C. Chen and Y.-G. Yao, S-nitrosoglutathione reductase alleviates morphine analgesic tolerance by restricting PKCα S-nitrosation, *Redox Biol.*, 2024, **75**, 103239, DOI: 10.1016/j.redox.2024.103239.

24 P.-Y. Ho, Y.-C. Koh, T.-J. Lu, P.-L. Liao and M.-H. Pan, Purple Napiergrass (Pennisetum purpureum Schumach) Hot Water Extracts Ameliorate High-Fat Diet-Induced Obesity and Metabolic Disorders in Mice, *J. Agric. Food Chem.*, 2023, **71**, 20701–20712, DOI: 10.1021/acs.jafc.3c05678.

25 B. Bertani, N. Ruiz and J. M. Slauch, Function and Biogenesis of Lipopolysaccharides, *EcoSal Plus*, 2018, **8**, DOI: 10.1128/ecosalplus.esp-0001-2018.

26 Y. Li, Z. Lu, L. Zhang, C. L. Kirkwood, K. L. Kirkwood, M. F. Lopes-Virella and Y. Huang, Inhibition of acid sphingomyelinase by imipramine abolishes the synergy between metabolic syndrome and periodontitis on alveolar bone loss, *J. Periodontal Res.*, 2021, **57**, 173–185, DOI: 10.1111/jre.12951.

27 Á. González-Domínguez, T. Belmonte, J. Domínguez-Riscart, P. Ruiz-Ocaña, I. Muela-Zarzuela, A. Saez-Benito, R. Montañez-Martínez, R. M. Mateos and A. M. Lechuga-Sancho, Altered insulin secretion dynamics relate to oxidative stress and inflammasome activation in children with obesity and insulin resistance, *J. Transl. Med.*, 2023, **21**, 559, DOI: 10.1186/s12967-023-04337-7.

28 T. Mezza, G. Muscogiuri, G. P. Sorice, G. Clemente, J. Hu, A. Pontecorvi, J. J. Holst, A. Giaccari and R. N. Kulkarni, Insulin resistance alters islet morphology in nondiabetic humans, *Diabetes*, 2014, **63**, 994–1007, DOI: 10.2337/db13-1013.

29 M. Pan, Y. Deng, Y. Qiu, D. Pi, C. Zheng, Z. Liang, J. Zhen, W. Fan, Q. Song, J. Pan, Y. Li, H. Yan, Q. Yang and Y. Zhang, Shenling Baizhu powder alleviates non-alcoholic fatty liver disease by modulating autophagy and energy metabolism in high-fat diet-induced rats, *Phytomedicine*, 2024, **130**, 155712–155728, DOI: 10.1016/j.phymed.2024.155712.

30 G. F. Grabner, H. Xie, M. Schweiger and R. Zechner, Lipolysis: cellular mechanisms for lipid mobilization from fat stores, *Nat. Metab.*, 2021, **3**, 1445–1465, DOI: 10.1038/s42255-021-00493-6.

31 Y. Yano, X. Hua, Y. Wan, S. Suman, B. Zhu, C. L. Dagnall, A. Hutchinson, K. Jones, B. D. Hicks, J. Shi, C. C. Abnet and E. Vogtmann, Comparison of Oral Microbiota Collected Using Multiple Methods and Recommendations for New Epidemiologic Studies, *mSystems*, 2020, **5**, e00156–20, DOI: 10.1128/mSystems.

32 Y. Wakita, Y. Shimomura, Y. Kitada, H. Yamamoto, Y. Ohashi and M. Matsumoto, Taxonomic classification for microbiome analysis, which correlates well with the metabolite milieu of the gut, *BMC Microbiol.*, 2018, **18**, 188, DOI: 10.1186/s12866-018-1311-8.

33 E.-J. Song, N. R. Shin, S. Jeon, Y.-D. Nam and H. Kim, Impact of the herbal medicine, Ephedra sinica stapf, on gut microbiota and body weight in a diet-induced obesity model, *Front. Pharmacol.*, 2022, **13**, 1042833, DOI: 10.3389/fphar.2022.1042833.

34 J. Ouyang, J. Lin, S. Isnard, B. Fombuena, X. Peng, A. Marette, B. Routy, M. Messaoudene, Y. Chen and J.-P. Routy, The Bacterium Akkermansia muciniphila: A Sentinel for Gut Permeability and Its Relevance to HIV-Related Inflammation, *Front. Immunol.*, 2020, **11**, 645, DOI: 10.3389/fimmu.2020.00645.

35 P. Paone, F. Suriano, C. Jian, K. Korpela, N. M. Delzenne, M. Van Hul, A. Salonen and P. D. Cani, Prebiotic oligofructose protects against high-fat diet-induced obesity by changing the gut microbiota, intestinal mucus production, gly-

cosylation and secretion, *Gut Microbes*, 2022, **14**, 2152307–2152330, DOI: **10.1080/19490976.2022.2152307**.

36 J. Chen, J. Liu, C. Yan, C. Zhang, W. Pan, W. Zhang, Y. Lu, L. Chen and Y. Chen, Sarcodon aspratus polysaccharides ameliorated obesity-induced metabolic disorders and modulated gut microbiota dysbiosis in mice fed a high-fat diet, *Food Funct.*, 2020, **11**, 2588–2602, DOI: **10.1039/c9fo00963a**.

37 L. Wang, P. Zhang, C. Li, F. Xu and J. Chen, A polysaccharide fromRosa roxburghiiTratt fruit attenuates high-fat diet-induced intestinal barrier dysfunction and inflammation in mice by modulating the gut microbiota, *Food Funct.*, 2022, **13**, 530–547, DOI: **10.1039/d1fo03190b**.

38 J. Ji, S. Zhang, M. Yuan, M. Zhang, L. Tang, P. Wang, Y. Liu, C. Xu, P. Luo and X. Gao, Fermented Rosa Roxburghii Tratt Juice Alleviates High-Fat Diet-Induced Hyperlipidemia in Rats by Modulating Gut Microbiota and Metabolites, *Front. Pharmacol.*, 2022, **13**, 883629–883641, DOI: **10.3389/fphar.2022.883629**.

39 L. Wang, C. Li, Q. Huang and X. Fu, Polysaccharide from Rosa roxburghii Tratt Fruit Attenuates Hyperglycemia and Hyperlipidemia and Regulates Colon Microbiota in Diabetic db/db Mice, *J. Agric. Food Chem.*, 2019, **68**, 147–159, DOI: **10.1021/acs.jafc.9b06247**.

40 Y. R. Lee, H.-B. Lee, M.-J. Oh, Y. Kim and H.-Y. Park, Thyme Extract Alleviates High-Fat Diet-Induced Obesity and Gut Dysfunction, *Nutrients*, 2023, **15**, 5007–5020, DOI: **10.3390/nu15235007**.

41 A. Morissette, C. Kropp, J.-P. Songpadith, R. Junges Moreira, J. Costa, R. Mariné-Casadó, G. Pilon, T. V. Varin, S. Dudonné, L. Boutekrabt, P. St-Pierre, E. Levy, D. Roy, Y. Desjardins, F. Raymond, V. P. Houde and A. Marette, Blueberry proanthocyanidins and anthocyanins improve metabolic health through a gut microbiota-dependent mechanism in diet-induced obese mice, *Am. J. Physiol.: Endocrinol. Metab.*, 2020, **318**, E965–E980, DOI: **10.1152/ajpendo.00560.2019**.

42 B. Saad, A Review of the Anti-Obesity Effects of Wild Edible Plants in the Mediterranean Diet and Their Active Compounds: From Traditional Uses to Action Mechanisms and Therapeutic Targets, *Int. J. Mol. Sci.*, 2023, **24**, 12641–12664, DOI: **10.3390/ijms241612641**.

43 F. Qian, B. Ouyang, Z. Cai, D. Zhu, S. Yu, J. Zhao, N. Wei, G. Wang, L. Wang and J. Zhang, Compound Shouwu Jiangzhi Granule regulates triacylglyceride synthesis to alleviate hepatic lipid accumulation, *Phytomedicine*, 2024, **129**, 155691–155700, DOI: **10.1016/j.phymed.2024.155691**.

44 D. Zeevi, T. Korem, N. Zmora, D. Israeli, D. Rothschild, A. Weinberger, O. Ben-Yacov, D. Lador, T. Avnit-Sagi, M. Lotan-Pompan, J. Suez, J. A. Mahdi, E. Matot, G. Malka, N. Kosower, M. Rein, G. Zilberman-Schapira, L. Dohnalová, M. Pevsner-Fischer, R. Bikovsky, Z. Halpern, E. Elinav and E. Segal, Personalized Nutrition by Prediction of Glycemic Responses, *Cell*, 2015, **163**, 1079–1094, DOI: **10.1016/j.cell.2015.11.001**.

45 J. H. Wang, S. J. Hwang, Y. J. Choi, T. W. Woo and C. G. Son, Lactobacillus casei–fermented Amomum xanthioides ameliorates metabolic dysfunction in high–fat diet–induced obese mice, *FASEB J.*, 2024, **38**, 23669–23680, DOI: **10.1096/fj.202400552R**.

46 Z. Li, B. Zhang, N. Wang, Z. Zuo, H. Wei and F. Zhao, A novel peptide protects against diet-induced obesity by suppressing appetite and modulating the gut microbiota, *Gut*, 2023, **72**, 686–698, DOI: **10.1136/gutjnl-2022-328035**.

47 T. Zhang, J. Liu, S. Shen, Q. Tong, X. Ma and L. Lin, SIRT3 promotes lipophagy and chaperon-mediated autophagy to protect hepatocytes against lipotoxicity, *Cell Death Differ.*, 2019, **27**, 329–344, DOI: **10.1038/s41418-019-0356-z**.

48 M. Zhao, Z. Jiang, H. Cai, Y. Li, Q. Mo, L. Deng, H. Zhong, T. Liu, H. Zhang, J. X. Kang, F. Feng, L. M. Cox and M. G. D. Bello, Modulation of the Gut Microbiota during High-Dose Glycerol Monolaurate-Mediated Amelioration of Obesity in Mice Fed a High-Fat Diet, *mBio*, 2020, **11**, 20–38, DOI: **10.1128/mBio.00190-20**.

49 H. Jian, Y. Liu, X. Wang, X. Dong and X. Zou, Akkermansia muciniphila as a Next-Generation Probiotic in Modulating Human Metabolic Homeostasis and Disease Progression: A Role Mediated by Gut–Liver–Brain Axes?, *Int. J. Mol. Sci.*, 2023, **24**, 3900, DOI: **10.3390/ijms24043900**.

50 P. D. Cani, C. Depommier, M. Derrien, A. Everard and W. M. de Vos, Akkermansia muciniphila: paradigm for next-generation beneficial microorganisms, *Nat. Rev. Gastroenterol. Hepatol.*, 2022, **19**, 625–637, DOI: **10.1038/s41575-022-00631-9**.

51 W. Wu, W. Kaicen, X. Bian, L. Yang, S. Ding, Y. Li, S. Li, A. Zhuge and L. Li, Akkermansia muciniphilaalleviate-shigh–fat–diet–related metabolic–associated fatty liver disease by modulating gut microbiota and bile acids, *Microb. Biotechnol.*, 2023, **16**, 1924–1939, DOI: **10.1111/1751-7915.14293**.